J|A|C|S
ARTICLES
Published on Web 04/22/2006

Dynamical Valence Fluctuation at the Charge−Density−Wave Phase Boundary in Iodide-Bridged Pt Compound $[Pt(chxn)_2I]I_2$

Shinya Takaishi,*,† Daisuke Kawakami,† Masahiro Yamashita,*,† Mari Sasaki,‡ Takashi Kajiwara,† Hitoshi Miyasaka,‡ Ken-ichi Sugiura,‡ Yusuke Wakabayashi,§ Hiroshi Sawa,§ Hiroyuki Matsuzaki,|| Hideo Kishida,|| Hiroshi Okamoto,|| Harutaka Watanabe,⊥ Hisaaki Tanaka,⊥ Kazuhiro Marumoto,⊥ Hiroshi Ito,⊥ and Shin-ichi Kuroda⊥

Contribution from the Department of Chemistry, Graduate School of Science, Tohoku University and CREST (JST), 6-3 Aza-aoba, Aramaki, Sendai 980-8578, Japan, Department of Chemistry, Graduate School of Science, Tokyo Metropolitan University, 1-1 Minamiosawa, Hachioji 192-0397, Japan, Institute of Materials Structure Science, High Energy Accelerator ResearchOrganization, Tsukuba 305-0801, Japan, Department of Advanced Materials Science, Graduate School of Frontier Sciences, The University of Tokyo, Kashiwa 277-8561, Japan, and Department of Applied Physics, Graduate School of Engineering, Nagoya University, Furocho, Chikusa-ku, Nagoya 464-8603, Japan

Received January 10, 2006; E-mail: takaishi@agnus.chem.tohoku.ac.jp; yamasita@agnus.chem.tohoku.ac.jp

Abstract: We synthesized a novel iodo-bridged linear chain platinum compound, having the quasi-two-dimensional charge−density−wave (CDW) ground state and the smallest band gap. In this compound, we discovered an anomalous valence state in the boundary region at which the CDW phase alternates in the crystal by means of ESR, X-ray diffuse scattering, STM, and electrical resistivity. This anomalous state can be explained by the fast fluctuation between $Pt^{IV}-I\cdots Pt^{II}$ and $Pt^{II}\cdots I-Pt^{IV}$ in the double well potential. This is the first observation of the dynamical fluctuation of the CDW phase among the quasi one-dimensional halogen-bridged complexes.

Introduction

One-dimensional (1D) electronic systems have been attracting much attention from the viewpoint of both pure and applied sciences. These systems are very promising for the application of nonlinear optical and nano-electronic devices, while from the viewpoint of pure sciences, many characteristic physical properties have so far been observed, for example, Mott−Hubbard, charge−density−wave (CDW), and spin−density−wave (SDW) states in organic (semi) conductors,[1−3] and nonlinear excitations such as solitons and polarons in π-conjugated polymers.[4,5] Among the 1D system, the halogen-bridged metal complexes also have been of recent interest because of the variety of their electronic states and many attractive physical properties such as intense charge-transfer bands,[6] overtone progressions of the resonance Raman spectra,[7] intense luminescence spectra with large Stokes shifts,[8] photogeneration[9] and long-range migration[10] of solitons and polarons, and large third-order optical nonlinearity,[11] as well as providing 1D model compounds of high T_c copper oxides superconductors, etc.

Theoretically, this system has been extensively studied by the extended Peierls−Hubbard model,[12,13] where the electron−phonon interaction (S), electron transfer (t), and on-site and nearest neighbor-site Coulomb repulsion energies (U and V, respectively) compete or cooperate with each other. It has been established that the Ni compounds take the Ni^{III} averaged-valence or Mott−Hubbard states, due to the strong on-site Coulomb repulsion, where the bridging halide ions are located at the midpoints between the neighboring two metal ions. In this case, the half-filled metallic band splits into the lower- and upper-Hubbard bands composed of a $Ni^{III}d_{z^2}$ orbital with the Hubbard gap of ca. 5 eV. Therefore, all Ni compounds belong to the class III category for the mixed-valence compounds

† Tohoku University.
‡ Tokyo Metropolitan University.
§ Institute of Materials Structure Science.
|| The University of Tokyo.
⊥ Nagoya University.

(1) Andrieux, A.; Jerome, D.; Bechgaard, K. *J. Phys. Lett.* **1981**, *42*, 87−90.
(2) Forro, L.; Bouffard, S.; Pouget, J. P. *J. Phys. Lett.* **1984**, *45*, 453−459.
(3) Hasegawa, T.; Kagoshima, S.; Mochida, T.; Sugiura, S.; Iwasa, Y. *Solid State Commun.* **1997**, *103*, 489−493.
(4) Goldberg, I. B.; Crowe, H. R.; Newman, P. R.; Heeger, A. J.; MacDiarmid, A. G. *J. Chem. Phys.* **1979**, *70*, 1132−1136.
(5) Su, W. P.; Schrieffer, J. R.; Heeger, A. J. *Phys. Rev. B* **1980**, *22*, 2099−2111.
(6) (a) Tanaka, M.; Kurita, S.; Kojima, T.; Yamada, Y. *Chem. Phys.* **1984**, *91*, 257−65. (b) Wada, Y.; Mitani, T.; Yamashita, M.; Koda, T. *J. Phys. Soc. Jpn.* **1985**, *54*, 3143−3153.
(7) Clark, R. J. H.; Franks, M. L.; Trumble, W. R. *Chem. Phys. Lett.* **1976**, *41*, 287−292.
(8) Tanino, H.; Kobayashi, K. *J. Phys. Soc. Jpn.* **1983**, *52*, 1446−1456.
(9) Okamoto, H.; Mitani, T.; Toriumi, K.; Yamashita, M. *Phys. Rev. Lett.* **1992**, *69*, 2248−2251.
(10) Kimura, N.; Ishimaru, S.; Ikeda, R.; Yamashita, M. *J. Chem. Soc., Faraday Trans.* **1998**, *94*, 3659−3663.
(11) Kishida, H.; Matsuzaki, H.; Okamoto, H.; Manabe, T.; Yamashita, M.; Taguchi, Y.; Tokura, Y. *Nature* **2000**, *405*, 929−932
(12) Okamoto, H.; et al. *Phys. Rev. B* **1996**, *54*, 8438−8445.
(13) Okamoto, H.; Toriumi, K.; Mitani, T.; Yamashita, M. *Phys. Rev. B* **1990**, *42*, 10381−10387.

10.1021/ja060193b CCC: $33.50

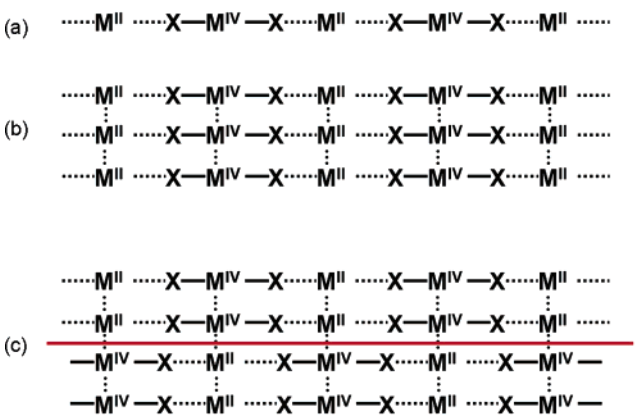

Figure 1. Schematic valence arrangement in halogen-bridged CDW compounds: (a) 1D-CDW, (b) 2D-CDW, and (c) CDW phase boundary in quasi-2D-CDW (red line).

proposed by Robin and Day.[14] On the other hand, the Pt and Pd compounds take the $M^{II}-M^{IV}$ mixed-valence or CDW states because of the strong electron−phonon interaction, where the bridging halide ions are displaced from the midpoints between the neighboring two metal ions. Accordingly, the half-filled metallic band splits into the occupied valence band composed of $M^{II}d_{z^2}$ and the unoccupied conduction band composed of $M^{IV}d_{z^2}$ with a finite Peierls gap. Therefore, Pt and Pd compounds belong to the Robin−Day's class II category.[14] These CDW compounds are classified into two categories depending on the strength of the interchain interaction, 1D-CDW and two-dimensional (2D)-CDW (Figure 1a and b, respectively).[15] In the 1D-CDW compounds, because no chemical bond exists between neighboring 1D chains, the CDW phase has no correlation between the neighboring chains. In the 2D-CDW compounds, on the other hand, because 1D chains are connected by the hydrogen bonds through the halide ions, the CDW is aligned with the same phase in a hydrogen-bonded 2D sheet. Recently, Wakabayashi et al. have revealed the spatial correlation of the CDW in $[Pd(chxn)_2Br]Br_2$ (chxn = 1*R*,2*R*-diaminocyclohexane) by means of an X-ray diffuse scattering.[16] They showed that even in the compound categorized into 2D-CDW, some compounds have no long-range but short-range charge order within a hydrogen-bonded 2D sheet as a consequent of the weak interchain interaction. Therefore, we represent such an electronic structure as "quasi-2D-CDW" in this paper. In the quasi-2D-CDW, a boundary region at which CDW phase is inverted must exist (Figure 1c). In this paper, we report a thermally generated anomalous electronic state in the boundary region of CDW phase inversion in the halogen-bridged Pt compound $[Pt(chxn)_2I]I_2$ having a quasi-2D-CDW ground state, evidenced by X-ray diffuse scattering, scanning tunneling microscopy (STM), electron spin resonance (ESR), and electrical resistivity.

Experimental Section

Crystals of $[Pt(chxn)_2I]I_2$ were synthesized by the slow diffusion of I_2 vapor into a methanol solution of $Pt(chxn)_2I_2$. X-ray crystal structure determination of $[Pt(chxn)_2I]I_2$ was made at 93 K using a Rigaku CCD diffractometer (Saturn 70) with graphite monochromated Mo Kα radiation ($\lambda = 0.7107$ Å). ESR spectra were measured by using a Bruker EMX spectrometer equipped with a gas-flow type cryostat Oxford ESR 900. An X-ray oscillation photograph and the intensity distribution of diffuse scattering were measured with the MacScience Imaging Plate diffractometer on the beam line 1B and Huber four-axes diffractometer on the beam line 4C combined with the synchrotron generated X-ray source installed in the photon factory of the High Energy Accelerator Research Organization. STM measurements were performed at room temperature and ambient pressure. Single crystals of $[Pt(chxn)_2I]I_2$ were cleaved and mounted onto a sample stage with carbon pastes so that the surface of the *bc* plane could be observed. The STM image was acquired with constant height mode using a JEOL JSPM-5200 microscope. A sample bias voltage (V_s) was chosen to be +1.1 V. The temperature dependence of electrical conductivity was measured using the four-probe dc method with a typical cooling rate of 1 K/min. The temperature was monitored with a calibrated Cernox resistor. The electrical leads were attached to a single crystal with carbon paste. The voltage appearing between the voltage leads was measured with an Agilent 34420A nanovoltmeter under a current of 0.1−0.01 μA supplied to the current leads from a YOKOGAWA 7651 programmable dc source. The measuring current was alternated to eliminate thermoelectric effects.

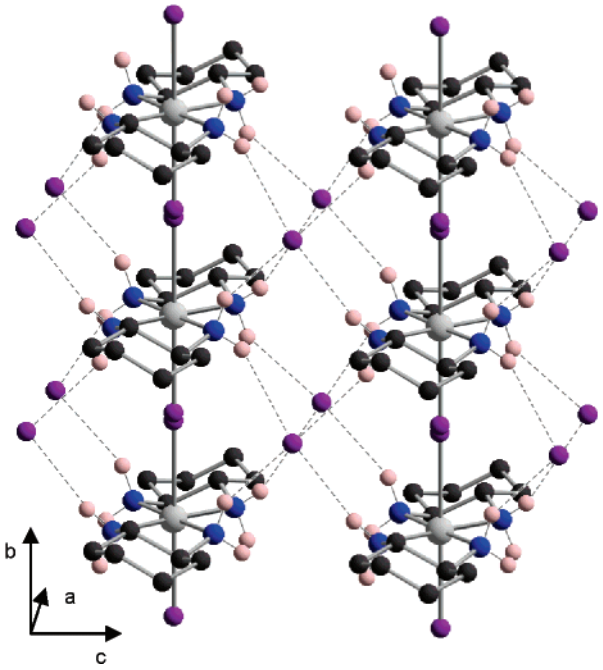

Figure 2. Perspective view of the crystal structure of $[Pt(chxn)_2I]I_2$ onto the *bc* plane. Gray, Pt; blue, N; black, C; and purple, I.

Results and Discussion

Figure 2 shows a perspective view of the crystal structure in $[Pt(chxn)_2I]I_2$ onto the *bc* plane determined at 93 K. The planar $[Pt(chxn)_2]$ moieties are bridged by the iodide ions, forming a linear chain structure. The linear chains are connected by the hydrogen bond between the hydrogen atoms of amino-group of chxn ligands and the counter iodide ions, forming 2D sheets. The bridging iodide ions are disordered with half occupancies at displaced position from the midpoints between the neighboring two Pt ions. This indicates that the present complex is in a $Pt^{II}-Pt^{IV}$ CDW state. The M−M distance *L*, the $Pt^{IV}-I$ distance l_1, and the $Pt^{II}\cdots I$ distance l_2 are 5.672, 2.716, and 2.956 Å, respectively. The distortion parameter (*d*) defined as $(l_2 - l_1)/L$ is evaluated to be 0.042, which is the smallest among all

(14) Robin, M. B.; Day, P. *Adv. Inorg. Radiochem.* **1967**, *10*, 247−422.
(15) Okamoto, H.; Yamashita, M. *Bull. Chem. Soc. Jpn.* **1998**, *71*, 2023−2039.
(16) Wakabayashi, Y.; Wakabayashi, N.; Yamashita, M.; Manabe, T.; Matsushita, N. *J. Phys. Soc. Jpn.* **1999**, *68*, 3948−3952.

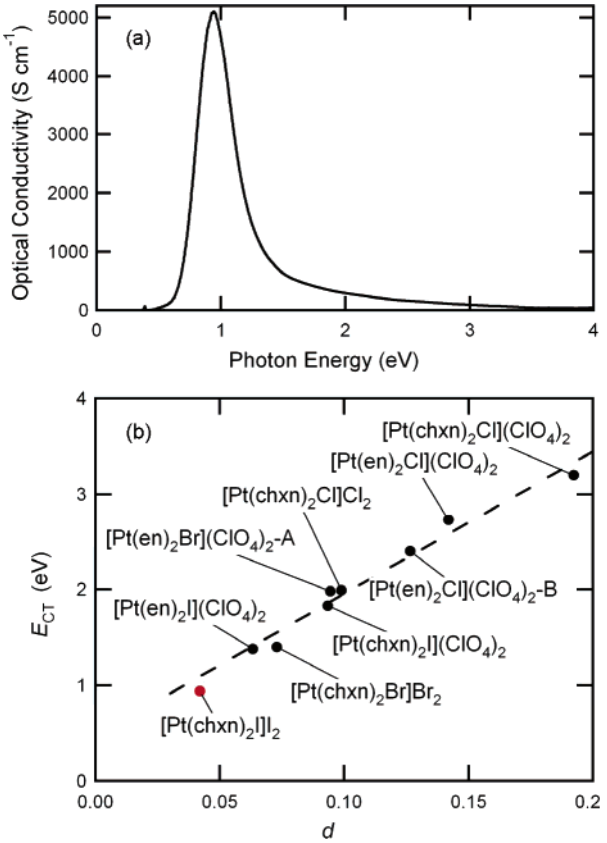

Figure 3. (a) Optical conductivity spectrum of $[Pt(chxn)_2I]I_2$. (b) CT energy of $[Pt(chxn)_2I]I_2$ together with those of representative halogen-bridged platinum complexes as a function of distortion parameter defined as $d = (l_2 - l_1)/L$, where L, l_1, and l_2 are the M−M distance, Pt^{IV}−I distance, and $Pt^{II}\cdots I$ distance, respectively. The broken line is merely to guide the eye.

halogen-bridged Pt compounds, indicating that the electronic state of this compound is most approaching the Pt^{III} Mott−Hubbard state.

Figure 3a shows the optical conductivity spectrum of the complex. The intense band was observed at 0.94 eV, which is attributable to the charge transfer from Pt^{II} to Pt^{IV} species. The charge-transfer energy (E_{CT}) of the present compound together with those of a series of halogen-bridged Pt complexes[15] is plotted as a function of those distortion parameters (d) in Figure 3b. The linear relationship between them is found. E_{CT} of the present complex is the smallest among all halogen-bridged Pt complexes, which is in good agreement with the crystal structure of the complex.

To clarify the charge arrangement in this compound, an X-ray diffuse scattering measurement was made. Wakabayashi et al. have revealed the spatial correlations of the charge arrangement of metal ions by observing diffused scattering in the halogen-bridged Pd complex $[Pd(chxn)_2Br]Br_2$.[16] According to this study, an X-ray diffuse scattering mainly originates in a displacement of the bridging halogen ions, which reflects the charge arrangement of the metal ions. Therefore, the information about the charge arrangements can be obtained also in the present complex. Figure 4a shows an oscillation photograph of $[Pt(chxn)_2I]I_2$ on the b^*c^* plane taken by a synchrotron-generated source at room temperature. Rod-shaped diffuse scatterings were observed along the a^* direction at $k = n + 1/2$ and $l = n$ position (n is an integer), which corresponds to the 2-fold periodicity along the b^* direction (chain direction). Therefore, it was

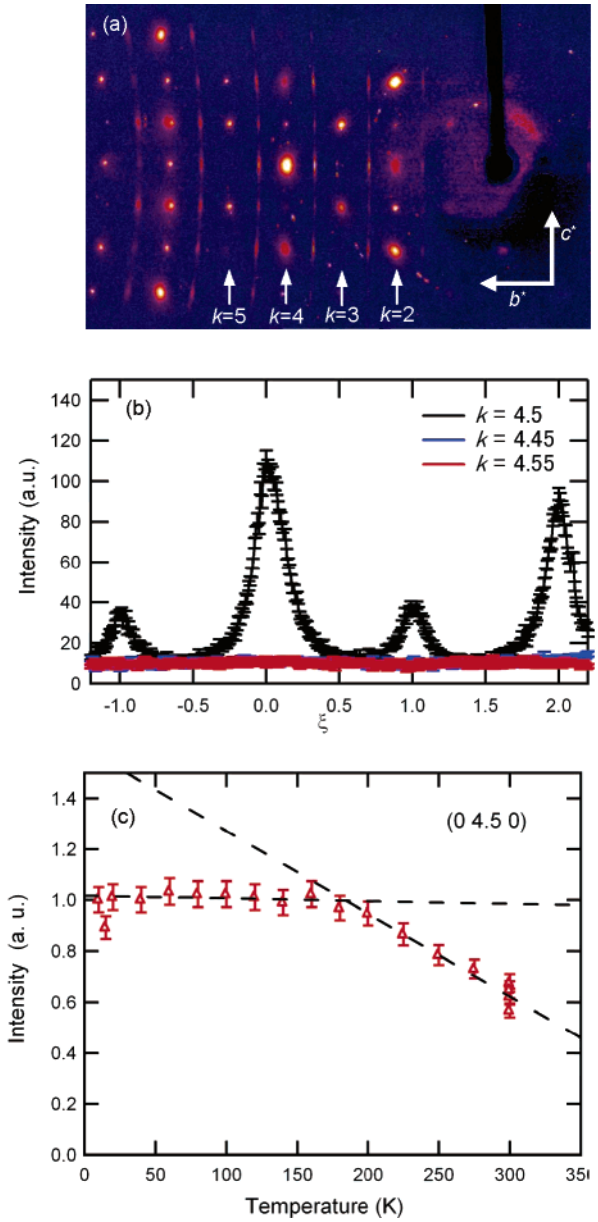

Figure 4. (a) Oscillation photograph of $[Pt(chxn)_2I]I_2$ on the b^*c^* plane. (b) Scattered X-ray intensity of $[Pt(chxn)_2I]I_2$ for (0 k ξ) line (k = 4.45, 4.5, 4.45) at room temperature. (c) Normalized intensity of X-ray diffuse scattering of $[Pt(chxn)_2I]I_2$ at (0 4.5 0) as a function of temperature.

clarified that CDWs have a correlation along the b and c axes and no correlation along the a axis. Figure 4b shows scattered X-ray intensity of $[Pt(chxn)_2I]I_2$ for the (0 4.5 ζ) line at room temperature. The intensity distribution in the c^* direction peaks at an integer value of ζ with the full width at half-maximum (fwhm) of approximately 0.25 reciprocal lattice units (r.l.u.), indicating that the CDW phase has a short-range order with the same phase along the c-axis. Therefore, this compound is in a quasi-2D-CDW state. Line width of this diffuse scattering showed almost no temperature dependence along any direction.

Figure 4c shows the peak intensity of X-ray diffuse scattering of $[Pt(chxn)_2I]I_2$ at (0 4.5 0) as a function of temperature. Below 180 K, the intensity is almost temperature independent, showing most of this compound is in the ground state, that is, $\cdots Pt^{II}\cdots I{-}Pt^{IV}{-}I\cdots Pt^{II}\cdots$ CDW state, in this temperature range. On the other hand, above 180 K, the intensity is gradually decreased

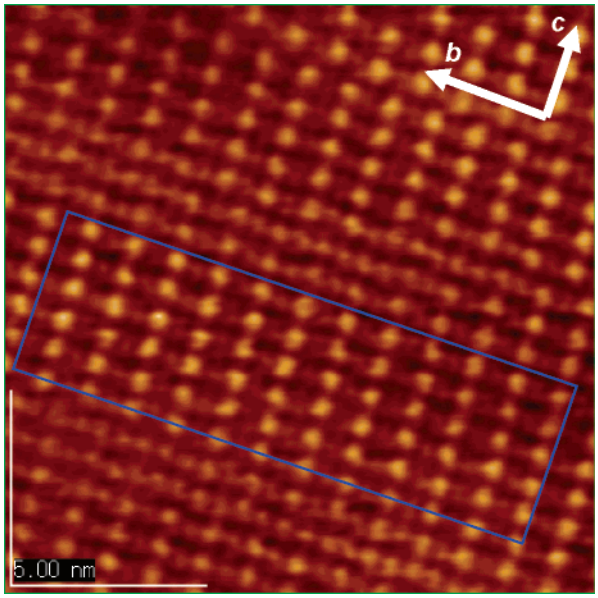

Figure 5. STM image of $[Pt(chxn)_2I]I_2$ at room temperature. Blue square shows the region in which the CDW phase is aligned with the same phase.

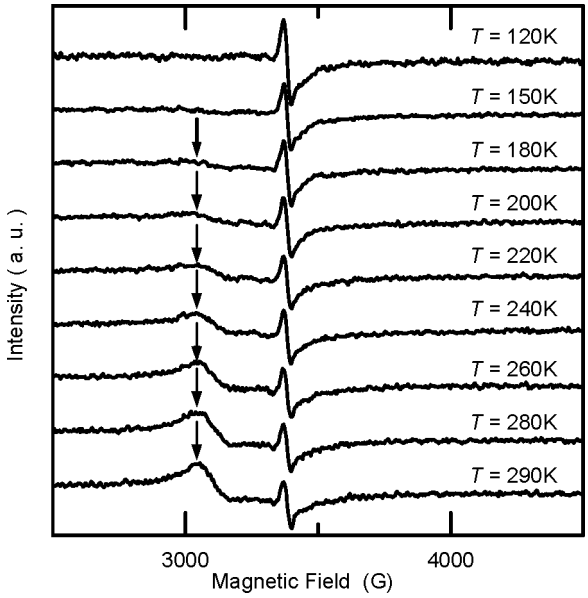

Figure 6. Temperature dependence of ESR spectrum in $[Pt(chxn)_2I]I_2$.

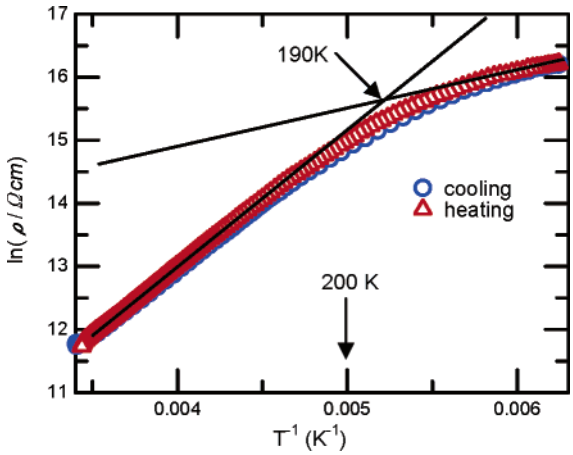

Figure 7. Arrhenius plot of electrical resistivity of $[Pt(chxn)_2I]I_2$. The solid lines are merely to guide the eye.

with increasing temperature, and that at 300 K is approximately 70% as intense as that at 180 K. Because the diffuse scattering intensity originates from the displacement of bridging halogen ions, this result indicates that approximately 30% of the chains afford no diffuse scattering at 300 K.

The STM technique is the powerful tool used to investigate the local valence structures. We have recently succeeded in visualizing the local electronic structure of halogen-bridged Ni−Pd mixed metal compounds by STM.[17] An STM measurement was then performed in the present compound to clarify the local electronic state. Figure 5 shows an STM image of $[Pt(chxn)_2I]I_2$ on the *bc* plane at room temperature. In the blue square of Figure 5, the bright spots were observed approximately every 11 Å along the chain, which reflects the 2-fold periodicity of the complex due to the CDW state. Because this STM image was acquired with positive sample bias, these bright spots indicate the tunnel current from Fermi energy (E_F) of the tip to the conduction band of the sample, which is composed of the d_{z^2} orbital of Pt^{IV} species. The bright spots are arranged along the *c*-axis approximately every 7 Å over 5 or 6 sites, indicating the CDW phase has a short-range order along the *c*-axis with the same phase, which is consistent with the X-ray diffuse scattering result. It is noteworthy that in the boundary region at which the CDW phase inverts, the bright spots are observed approximately every 5.5 Å along the chain. This area reaches 30% of the whole area, which is in good agreement with the decreased ratio of X-ray diffuse scattering intensity.

From this finding and the X-ray diffuse scattering result, we can lead to the two possible electronic states at the CDW phase boundary. One possible state is the formation of a static $-Pt^{III}-I-Pt^{III}-I-Pt^{III}-$ averaged-valence state. In this state, no diffuse scattering should be observed because bridging iodide ions are located at the midpoint between neighboring Pt ions. The other possibility is the dynamical fluctuation between Pt^{II} and Pt^{IV} states. In this situation, the CDW correlation along the chain should be broken, resulting in a broadening of the diffuse scattering peaks. Furthermore, if the fluctuation rate is much faster than the STM time scale, this state should afford an STM image similar to that of the $-Pt^{III}-I-Pt^{III}-I-Pt^{III}-$ averaged-valence state.

To obtain information about the thermally excited state, X-band ESR measurements were made. Figure 6 shows the temperature dependence of ESR spectra in the present compound (polycrystalline sample). Below 180 K, almost no ESR signal was observed (the signal around 3300 G ($g = 2.0$) is of extrinsic origin). This indicates that $[Pt(chxn)_2I]I_2$ takes $M^{II}-M^{IV}$ mixed-valence or CDW states. The signal was slightly observed at 190 K around 3000 G ($g = 2.2$) and became larger with increasing temperature. This ESR signal is characteristic of the anisotropic signal ($g_\perp$) from an unpaired electron located on the d_{z^2} orbital. Such a result indicates the existence of thermally generated Pt^{III} ($S = {}^1/_2$) species in the crystal. Because such a temperature dependence is very similar to that of X-ray diffuse scattering, one may assume that Pt^{III} species observed in ESR spectra should be the origin of the decrease of X-ray diffuse scattering intensity. However, a spin concentration is shown to be on the order of 0.01% at 300 K, which is much less than the 30% expected from the X-ray diffuse scattering and STM. If

(17) Takaishi, S.; et al. *Angew. Chem., Int. Ed.* **2004**, *43*, 3171−3175.

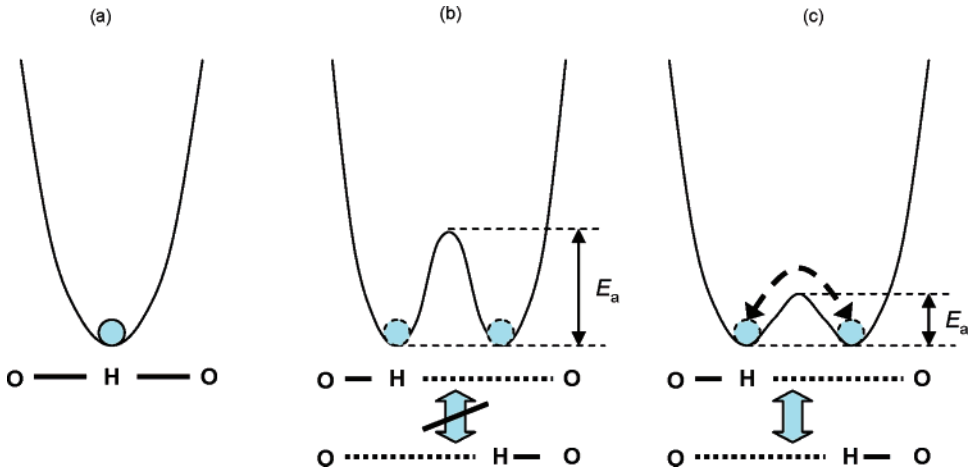

Figure 8. Three possible configuration coordinations in the O−H···O hydrogen-bonded system.

we assume that the 1D order of the $-Pt^{III}-I-Pt^{III}-I-Pt^{III}-$ chain is formed at the CDW phase boundary, the magnetic moment may be suppressed by the strong antiferromagnetic interaction. In this case, however, the J/k_B value (k_B is the Boltzmann constant) is evaluated to be 5×10^4 K by fitting the Eggert−Affleck−Takahashi (EAT) theoretical curve[18] to the experimental spin susceptibility, which seems to be too large to assume. Therefore, the observed ESR spectra originate from the small amount of the isolated Pt^{III} state. Thermal excitation of such a paramagnetic species has been discussed on the basis of the spin soliton model in $[Pd(chxn)_2]Br_2$.[13] If the fast fluctuation between Pt^{II} and Pt^{IV} states occurs, a small amount of soliton-like Pt^{III} species may be created coincidentally as detected by the present ESR measurement.

Figure 7 shows the Arrhenius plot of the electrical resistivity of the present complex. At room temperature, the conductivity was on the order of 10^{-4} S/cm. This complex showed a semiconductor-like behavior. The activation energy changed at approximately 190 K. It was evaluated to be 0.16 and 0.28 eV below 180 K and above 200 K, respectively. Because the activation energies are smaller than the optical gap, the conduction is considered to occur via impurity sites. The temperature at which the activation energy changes agrees with that at which ESR signals begin to appear. Because the electrical resistivity at room temperature is smaller than the resistivity extrapolated from the low-temperature region, some kind of conducting carrier is generated above 190 K.

Here, we consider the potential curve of the $Pt^{IV}-I\cdots Pt^{II}$ system. A similar example is the case of the O−H···O hydrogen-bonded system, which has been widely studied in solid-state chemistry and physics.[19] In this system, the feature of potential curve is classified into the three types depending on the O−O distance.[20] In case of a short O−O distance (d(O−O) < 2.5 Å), the hydrogen atom is located at the midpoint between neighboring oxygen atoms, as a consequence of a single well potential (Figure 8a). In case of a long O−O distance (d(O−O) > 2.7 Å), double well potential is formed and the hydrogen atom is located at the displaced position from the midpoint. In this case, the activation energy (E_a) is too high to be thermally activated ($E_a \gg k_BT$) for the hydrogen atom motion (Figure 8b). In case of a intermediate O−O distance (2.5 Å < d(O−O) < 2.7 Å), double well potential is also formed. However, the activation energy is comparable to the thermal energy ($E_a \approx k_BT$), and hydrogen atoms can move between two sites overcoming the activation energy (Figure 8c).

In the halogen-bridged complexes, the three potential curves are also possible depending on metal−metal distances. However, in all Pt and Pd compounds so far reported, bridging halide ions are statically disordered, indicating that these compounds belong to the second type ($E_a \gg k_BT$). In the present compound, the shape of the potential curve at the boundary region of the CDW phase should be the double well, $Pt^{IV}-I\cdots Pt^{II}$, because the decrease of the diffuse scattering intensity and the increase of the ESR signal are thermally induced. Therefore, we concluded that the fast exchange between $Pt^{IV}-I\cdots Pt^{II}$ and $Pt^{II}\cdots I-Pt^{IV}$ occurs at the boundary region of the CDW phase in the present compound as a consequence of the third type ($E_a \approx k_BT$) of potential curve. The reason for such an anomalous behavior can be recognized as follows. This compound originally has the smallest Pt−Pt distance and the lowest optical gap. Furthermore, the CDW is destabilized because Pt ions at the boundary are surrounded by Pt^{II} and Pt^{IV} states.

Here, we discuss the rate of the valence fluctuation between $Pt^{IV}-I\cdots Pt^{II}$ and $Pt^{II}\cdots I-Pt^{IV}$. Although it is quite difficult to determine the fluctuation rate itself, we can estimate it by assuming that the valence fluctuation and the hopping motion of the paramagnetic Pt^{3+} species have the same time scale. An ESR is a useful method to determine the dynamics of such a paramagnetic species.

By assuming the hopping motion of paramagnetic Pt^{3+} species, the line width of the ESR spectrum is shown by the concept of motional narrowing, and the following equation, [21]

$$\Delta\omega \approx \omega_p^2/\omega_e$$

where $\Delta\omega$, ω_p, and ω_e are the line width of the spectrum, the static line width that is mainly determined by the hyperfine coupling, and the hopping frequency of the paramagnetic

(18) Eggert, S.; Affleck, I.; Takahashi, M. *Phys. Rev. Lett*. **1994**, *73*, 332−335.
(19) (a) Moritomo, Y.; Tokura, Y.; Takahashi, H.; Môri, N. *Phys. Rev. Lett*. **1991**, *67*, 2041−2044. (b) Dalal, N.; Klymachyov, A.; Bussmann-Holder, A. *Phys. Rev. Lett.* **1998**, *81*, 5924−5927. (c) Terao, H.; Sugawara, T.; Kita, Y.; Sato, N.; Kaho, E.; Takeda, S. *J. Am. Chem. Soc.* **2001**, *123*, 10468−10474.
(20) (a) Hamilton, W. C.; Ibers, J. A. *Hydrogen Bonding in Solid*; W. A. Benjamin, Inc.: New York, 1968. (b) Scheiner, S. In *Proton Transfer in Hydrogen-Bonded Systems*; Bountis, T., Ed.; Premium Press: New York, 1992; pp 29−47.
(21) Anderson, P. W.; Weiss, P. R. *Rev. Mod. Phys.* **1953**, *25*, 269−276.

species, respectively. We measured the ESR spectra using a large amount of polycrystalline samples (Figure S1) and succeeded in observing a broad spectrum (340 ± 50 G) at 5 K, which is attributable to the signal of static Pt^{3+} species (ω_p). On the other hand, a sharp spectrum (160 ± 20 G) was observed at 290 K. By analyzing these spectra, we evaluated the hopping rate of 2×10^9 Hz at 290 K, which is consistent with the finding that the valence fluctuation is much faster than the STM time scale.

In summary, we discovered an anomalous valence state at the boundary region of CDW phase alternation in quasi 1D-iodide-bridged platinum complex $[Pt(chxn)_2I]I_2$, having the smallest band gap, by means of ESR, X-ray diffuse scattering, STM, and electrical resistivity. This state can be explained by the fast fluctuation between $Pt^{IV}-I\cdots Pt^{II}$ and $Pt^{II}\cdots I-Pt^{IV}$ in the double well potential. This is the first observation of the dynamic disorder of the CDW phase among the quasi-one-dimensional halogen-bridged complexes.

Acknowledgment. We acknowledge Prof. Iwano at the Institute of Materials Structure Science for helpful discussions. This work was partly supported by a Grant-in-Aid for Creative Scientific Research from the Ministry of Education, Culture, Sports, Science, and Technology.

Supporting Information Available: Complete refs 12 and 17, X-ray crystallographic information of the present compound in CIF format, and ESR spectra with a large amount of polycrystalline sample. This material is available free of charge via the Internet at http://pubs.acs.org.

JA060193B